



Antibacterial cellulose membrane via one-step covalent immobilization of ammonium/amine groups



Jianqiang Meng^{a,*}, Xin Zhang^a, Lei Ni^a, Zhuo Tang^b, Yufeng Zhang^a, Yongjun Zhang^b, Wen Zhang^a

^a State Key Laboratory of Hollow Fiber Membrane Materials and Processes, Tianjin Polytechnic University Tianjin 300387, China

^b Key Laboratory of Functional Polymer Materials, Institute of Polymer Chemistry, College of Chemistry, Nankai University, Tianjin 300071, China

HIGHLIGHTS

- Antibacterial cellulose membranes were prepared via alkoxy silane polycondensation.
- RC-QASC18 and RC-NH₂ membranes have a bacteria killing ratio over 99.5%.
- RC-QASC18 and RC-NH₂ membranes have a strong bacteria-adhesion property.
- An adjacent hydrophobic alkyl group is required for antibacterial property.
- The antibacterial property is robust in a wide range of pH and temperature.

ARTICLE INFO

Article history:

Received 27 September 2014

Received in revised form 5 December 2014

Accepted 21 December 2014

Available online xxxx

Keywords:

Antibacterial

Cellulose membrane

Alkoxy silane polycondensation

Bacteria anti-adhesion

ABSTRACT

This work describes a direct covalent linking of quaternary ammonium salts (QAS) and aminoalkyl groups onto regenerated cellulose (RC) membrane surface to prepare contact active antibacterial membrane materials. The membranes were prepared via alkoxy silane polycondensation reaction with three silane coupling agents, including trimethoxysilylpropyl trimethyl ammonium chloride (QAS_{CO}), trimethoxysilylpropyl octadecyldimethyl ammonium chloride (QAS_{C18}) and 3-aminopropyltrimethoxysilane (APS). FTIR, XPS, FESEM and AFM were used to characterize the chemical composition and surface morphology of the resulted RC-QAS_{CO}, RC-QAS_{C18} and RC-NH₂ membranes. Membrane surface charge properties were measured by the streaming potential method. Static water contact angle (WCA) and permeation flux were measured to investigate surface wettability and membrane permeability. *Escherichia coli* and *Staphylococcus aureus* were used as model bacteria to evaluate the antibacterial properties of membranes. The bacterial cell viability on membrane surfaces was evaluated by the dynamic shake flask test and the bacterial anti-adhesion properties were evaluated by confocal laser scanning microscopy (CLSM) measurements following the immersion test. RC-QAS_{C18} and RC-NH₂ membranes show strong antibacterial and bacteria anti-adhesion properties. Both membranes have a bacteria killing ratio over 99.5%. The stability study shows that the antibacterial property of modified membranes is robust in a wide range of pH and temperature conditions.

© 2014 Elsevier B.V. All rights reserved.

1. Introduction

In recent years, membrane technology has found industrial applications in a variety of advanced separation and purification processes due to its low energy consumption, easy operation, stable effluent quality, etc. As an advanced separation and purification technology, membrane technology has been widely used not only for wastewater treatment but also for biological processes such as protein separation, blood-cell separation and hemodialysis [1–4]. Among diverse membrane technologies, microfiltration is one of the most efficient methods used for primary

separation in biological production processes such as microbial cell removing, protein separation as well as blood purification [5,6].

As a major commercialized polymeric microfiltration membrane, cellulose membrane has been widely used in biotechnology fields because of its uniform porous structure, good hydrophilicity, good mechanical properties and biocompatibility [7,8]. However, the application of cellulose membrane is still limited by the fouling phenomena on the membrane surface, among which biofouling is mostly challenging, specifically for biological processes [9,10].

Biofouling is much more complicated than other types of membrane fouling. It can be divided into several stages, including early bacterial attachment, subsequent growth of bacteria on the membrane surface and then production of a gel-like substance by microorganisms (extracellular polymeric substances, EPS), which are responsible for adhesion

* Corresponding author.

E-mail address: jianqiang.meng@hotmail.com (J. Meng).

to material surfaces and building of three-dimensional architecture of the biofilm [11–17]. Many methods have been reported to improve the antibacterial and bacterial anti-adhesive properties of polymeric membranes. There are three common strategies to improve the antibacterial property of membrane surfaces [18]. The first approach is suppressing bacteria adhesion by creating superhydrophobic surfaces [19]. The second approach is biocide leaching with the incorporated toxic compounds released and diffuse over time from the material surface [20,21]. The third approach is contact killing via conjugation of the material surface with antibiotic functional groups such as quaternary ammonium salts, guanidine moieties and phosphonium salts [22–24]. Compared with the other two strategies, the synthesis of contact killing surfaces not only can effectively alter membrane surface properties, but also can significantly suppress bacterial growth in the fluid, without the release of active molecules leading to second contamination of the environment. Because of these advantages, the synthesis of contact killing surfaces attracts the most attention.

Cationic contact killing surfaces are now well recognized to have a powerful antimicrobial activity and strong biocidal effects against many bacteria species including both gram-negative bacteria and gram-positive bacteria. A number of papers have reported that cationic alkylammonium and alkylamine groups can be immobilized onto membrane surface to tailor membrane properties due to their good antibacterial properties, low toxicity, lack of skin irritation, good environmental stability, and good cell membrane penetration properties as well as good bacteria adhesion resistance [25–27]. Several techniques have been reported to immobilize cationic antibacterial groups onto membrane surfaces, including tethering antimicrobial polymers onto membrane surface via chemical coupling reactions, surface initiated polymerization of monomers having antibacterial moieties, and synthesis of surface-tethered antimicrobial polymer brush via post-polymerization modifications [28–32]. A major challenge for these methods is that the reaction processes are complex and multi-step.

In this study, antibacterial cellulose membranes were prepared by a one-step modification method based on alkoxy silane polycondensation reaction. Three commercial silane coupling agents including trimethoxysilylpropyl trimethyl ammonium chloride (QAS_{CO}), trimethoxysilylpropyl octadecyldimethyl ammonium chloride (QAS_{C18}) and 3-aminopropyltrimethoxysilane (APS) were used to anchor alkylammonium and alkylamine groups onto the membrane surface. The modified RC membranes were thoroughly characterized in terms of surface composition, morphology as well as antimicrobial activity and bacterial cell adhesion properties.

2. Experimental section

2.1. Materials

Regenerated cellulose (RC) membranes (diameter of 47 mm and average pore diameter of 0.45 μm) were purchased from Sartorius Stedim Biotech (Germany). Before surface modification, the membranes were washed with deionized water for 0.5 h and then freeze-dried to constant weight. Trimethoxysilylpropyl trimethyl ammonium chloride (QAS_{CO}), trimethoxysilylpropyl octadecyldimethyl ammonium chloride (QAS_{C18}), 3-aminopropyl-trimethoxysilane (APS, 97%) and acetone were purchased from J&K Chemical Co. (China). For the bacterial growth test, *Escherichia coli* (DH5α, gram-negative) and *Staphylococcus aureus* (ATCC 6538, gram-positive) were purchased from Shanghai BioRc Co., Ltd. Molecular Probes including Syto 9 and Syto propidium iodide (PI) were purchased from Jiamay Biotech Co. Ltd, Beijing. Phosphate buffered saline solution (PBS, pH 7.4) (8.0 g NaCl, 0.2 g KCl, 1.44 g Na₂HPO₄, 0.24 g KH₂PO₄) was prepared in house. Ethanol (95%) and acetic acid (99.5%) were purchased from Tianjin Kermel Chemical Reagent Co. Deionized (DI) water was obtained from a Millipore Milli-Q Advantage A10 water purification system (18.2 MΩ cm at 25 °C

1.2 μg/L TOC) (Billerica, MA, USA). All the other chemicals were used as received without further purification.

2.2. Synthesis of the antibacterial RC membranes

Antibacterial cellulose membranes were prepared via alkoxy silane polycondensation using three silane coupling agents. Scheme 1 shows the synthesis mechanism.

For the synthesis of RC-QAS membranes, trimethoxysilylpropyl trimethyl ammonium chloride (QAS_{CO}) (3.5 mL, 12 mmol) or trimethoxysilylpropyl octadecyldimethyl ammonium chloride (QAS_{C18}) (5 mL, 9 mmol) was added into DI water (10 mL) to obtain the QAS solution and was adjusted with acetic acid to pH 4.0. Then, the wet BC membranes (17.3 cm², 120 mg of dry cellulose) were immersed in this solution for 4 h with orbital stirring at 25 °C. The resulting RC membranes were vigorously washed with ethanol to remove the unreacted QAS_{CO}/QAS_{C18} and dried in a vacuum oven at 110 °C for 2 h. Thereafter, the sample was extensively extracted with ethanol (95%) in Soxhlet apparatus to remove the non-immobilized QAS_{CO}/QAS_{C18} and small molecule impurities. Finally, the membranes were freeze-dried to constant weight.

For the synthesis of RC-NH₂ membrane, a piece of wet RC membrane (17.3 cm², 120 mg of dry cellulose) was immersed in a previously prepared solution of 3-aminopropyltrimethoxysilane (APS) (5 mL, 25 mmol) in acetone (40 mL) and the mixture was gently stirred at 25 °C for 4 h. The modified RC membranes were then washed with acetone to remove the unreacted APS and other impurities. After being dried in a vacuum oven at 110 °C for 2 h, the RC-NH₂ samples were submitted to a Soxhlet extraction with acetone for 4 h and dried in a freeze dryer.

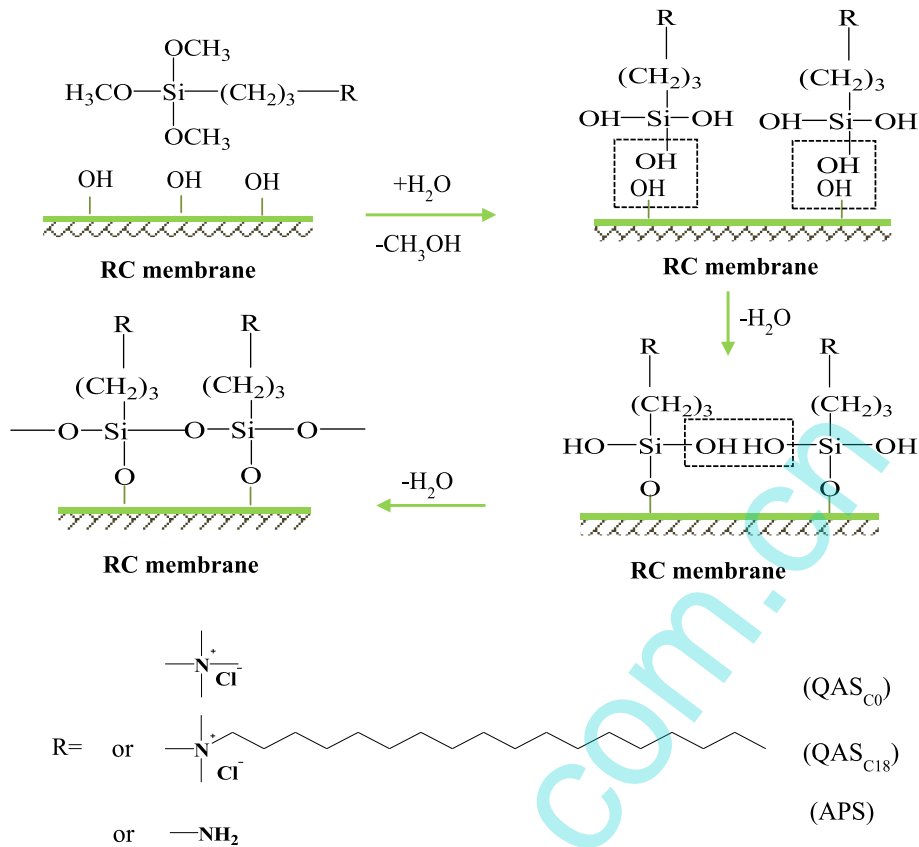
The grafting yield (mg/cm²) of each RC grafted membrane was calculated using the following equation (Eq. (1)):

$$GY = (m_1 - m_0) / A \quad (1)$$

where GY (mg/cm²) is the grafting yield, m₀ (mg) and m₁ (mg) represent the weight of the dried membrane before and after grafting, respectively, and A (cm²) is the area of the membrane.

2.3. Characterization of the modified RC membranes

The chemical structure of the RC membranes was investigated by FTIR spectroscopy (Bruker, Vector-22) with Zinc Selenide (ZnSe) as an internal reflection element at an incident angle of 45°. Each spectrum was collected in the range of 500–4000 cm⁻¹ by accumulating 32 scans at a resolution of 4 cm⁻¹. The surface composition of modified membranes was measured using XPS on a Quanta200 spectrometer (FEI Co. Ltd, USA) with a monochromatic Al Kα X-ray source (1486.6 eV photons) at a pass energy of 93.9 eV. The measurements were conducted at a take-off angle of 45°. Survey spectra were run in the binding energy range of 0–1000 eV, followed by a high-resolution scan of the N1s region. Binding energies were calibrated using the containment nitrogen (N1s = 402.3 eV). The membrane surface morphologies were observed by FESEM (Hitachi S-4800, Japan) under high vacuum condition. The accelerating voltage used was 5 kV. The membrane samples were first dried on a freeze dryer (FD-1A-50, Hanuo Instrument Co. Ltd, Shanghai), and then were mounted on sample stages using double-sided conductive tape and were sputter-coated with gold prior to FESEM measurements. Membrane surface morphologies were also measured by AFM (CSPM5500, Being Nano-Instruments, China) imaging and analysis, equipped with a standard silicon nitride cantilever. Membrane surface charge properties were evaluated using the streaming potential method. Measurements were carried out with a 0.01 mol/L KCl solution as a feed solution at 25 ± 1.0 °C. The pH was adjusted from 3.0 to 9.0 using hydrochloric acid and sodium hydroxide solutions. The membrane samples were equilibrated for at least 24 h in 0.01 mol/L KCl solution before test. Surface zeta potentials were calculated from the measured streaming potentials using the Helmholtz–Smoluchowski equation [33]. The WCA of the membrane



Scheme 1. Reaction mechanism of covalent linking of ammonium/amine groups onto RC membrane surface.

surface was analyzed with a Kruss Instrument (CM3250-DS3210, Germany) at 25 °C. One drop of water (1 μL , pH 7.14) was put on the membrane surface with an automatic piston syringe and photographed. Three locations were selected for measurements for each sample. The surface energy of the membranes was estimated from contact angle data using the Young–Dupré equation (Eq. (2)):

$$E = \gamma(1 + \cos\theta) \quad (2)$$

where E is the surface energy (mN/m), γ is the surface tension of water (7.28×10^{-2} N/m, 20 °C) and θ is the contact angle (°). The pore size distribution of the original and modified RC membranes was characterized by the mercury porosimetry method. Mercury porosimetry measurements were performed on an AutoPore IV-9500 (Micromeritics) in the pressure range of 1–33,000 psi. The samples were dried for 24 h (in an oven at 100 °C) prior to analysis.

2.4. Permeation flux measurements

Permeation experiments were conducted using a lab-scale unit containing a cross-flow testing cell. The effective area of the testing cell is 7.06 cm^2 and the temperature of feed solutions was maintained at 25 °C. Membrane samples were pre-compacted at 0.1 MPa by DI water for 30 min in order to get steady filtration. Then, the permeate volume was recorded for a predetermined time at 0.1 MPa. The membrane flux was calculated using the following equation (3):

$$F = V/(At) \quad (3)$$

where F is the water permeation flux ($\text{L}/\text{m}^2 \cdot \text{h}$), V is the permeate volume (L) at a predetermined time t (h) and A is the effective membrane area (m^2).

2.5. Antibacterial assay

The antibacterial properties of the original and modified membranes were evaluated by a shake flask test using *E. coli* as the model gram-negative bacteria and *S. aureus* as the model gram-positive bacteria [34]. The bacteria were cultivated in liquid lysogeny broth (LB) medium (containing 10 g/L peptone, 5 g/L yeast extract and 10 g/L sodium chloride, pH = 7.0) and then placed in an incubator-shaker overnight at 37 °C. Following that, the *E. coli* or *S. aureus* solution (1 mL) was pipetted from the overnight phase into another flask containing 50 mL of freshly prepared LB. The mixture was then cultured at 37 °C in an incubator shaker for another 5 h to obtain bacterial suspension at exponential growth phase. This was done because the bacterial suspension at exponential growth phase was believed to have higher activity and be more viable than other growth phases. Then, the bacterial suspension (*E. coli* or *S. aureus*) was diluted with the LB liquid culture medium to 1×10^6 colony forming units (CFU)/mL. 30 μL of the diluted bacterial suspension was pipetted out from the flask and spread onto the surfaces of original and modified membranes (area of 1.5 cm^2). After placing the membranes on the nutritive agar plate, the plates were sealed and incubated at 37 °C for 12 h. Finally, the numbers of the CFU on membrane surface were counted.

In order to further evaluate the antibacterial performance against *E. coli* and *S. aureus*, the membrane (5 cm^2) was immersed into the bacterial suspension (10 mL, 1×10^6 CFU/mL) in sealed bottles and the mixtures in the bottles were shaken in an incubator shaker at 120 rpm and 37 °C for 6 h. After that, CFU counting method was used to estimate the number of viable *E. coli* and *S. aureus* remained in the suspensions. Before the experiments, the membrane samples were sterilized with UV irradiation and all glass ware and plastics were sterilized by autoclaving. After incubating with the membranes, a 100 μL serial 10-fold dilutions was pipetted into freshly prepared agar plates. The agar plates were then incubated at 37 °C overnight and the bacteria colonies developed

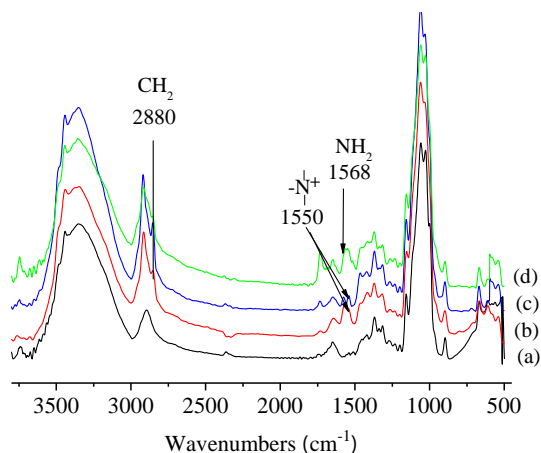


Fig. 1. FTIR spectra of regenerated cellulose (RC) (a), RC-QAS_{C0} (b), RC-QAS_{C18} (c) and RC-NH₂ (d) membranes.

were observed. Finally, the number of CFU was counted [35]. The bacteria killing ratio (sterilization ratio) was calculated by Eq. (4).

$$\text{Bacteria killing ratio}(\%) = ((N_B - N_S) / N_B) \times 100\% \quad (4)$$

where N_B and N_S are the number of colonies on the control plate and the sample plate, respectively. Each membrane sample was measured three times.

2.6. Bacterial anti-adhesion property measurements

The bacterial anti-adhesion property of the modified membranes was evaluated using a static adhesion test. At first, the original and modified membranes (5 cm²) were immersed in 8 mL of bacterial suspension (*E. coli* or *S. aureus*, 1 × 10⁶ CFU/mL) in a sealed bottle and the mixture was shaken in an incubator shaker at 120 rpm and 37 °C for 6 h. After that, the membranes were taken out, rinsed three times with NaCl solution (0.85 w/w%) and immersed in a staining solution for 15 min. The staining solution was composed of 1.5 μL of a cell-permeable green fluorescence dye (Syto 9) and 1.5 μL of a viable cell-impermeable red dye (Syto PI) in 1 mL of 0.85 w/w % NaCl solution. Then, each membrane sample was immersed into 2.5% (v/v) glutaraldehyde solution at 4 °C for 1 h to fix the adhered bacteria. Finally, the bacteria were examined using a LEICA TCS 700 Meta confocal laser scanning microscope (CLSM, 63 × oil objective). The green fluorescence and red fluorescence correspond to live and dead cells, respectively.

2.7. Stability study

In order to perform stability study of the modified membranes, the following aqueous solutions were prepared: (i) phosphoric acid solution at pH = 1.5, (ii) acetic acid solution at pH = 3.5, (iii) DI water at pH = 6.5 and (iv) triethylamine solution at pH = 10.8. The membrane (4 cm²) was immersed in 5 mL of the prepared solution in a sealed bottle and the mixture was shaken for 48 h at a predetermined temperature (25 °C, 50 °C and 90 °C). Finally, the antibacterial properties of each membrane were tested using the same procedure as described in Section 2.5. The diffusion inhibition zone test was also conducted to demonstrate the non-leaching property of antimicrobial substances.

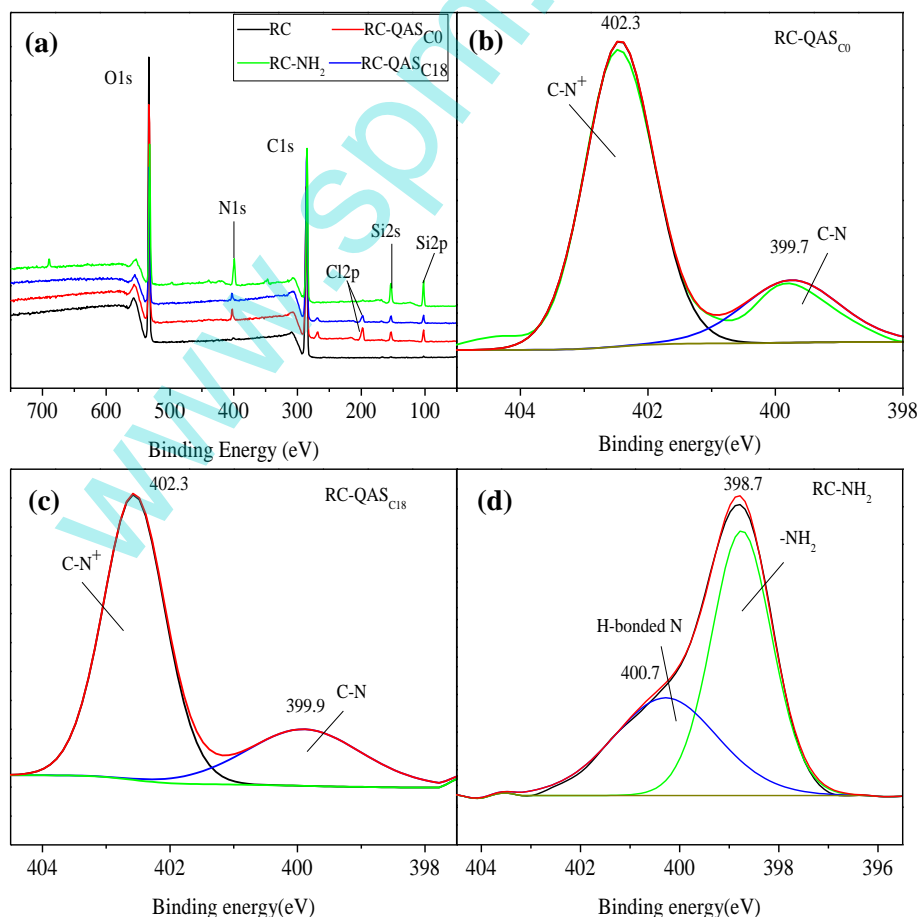


Fig. 2. XPS wide-scan spectra of original and modified RC membrane surfaces (a) and high-resolution XPS N 1s spectra of RC-QAS_{C0} (b), RC-QAS_{C18} (c) and RC-NH₂ (d) membranes.

Table 1
Elemental surface composition of RC and surface modified RC membranes determined from XPS.

Sample	Element (at.%)				
	C	O	Si	N	Cl
RC	56.07	43.93			
RC-QAS _{C0}	57.70	32.63	5.05	2.60	2.04
RC-QAS _{C18}	70.96	22.09	3.83	1.92	1.20
RC-NH ₂	59.74	21.45	6.17	11.20	

The diluted bacteria solution was placed on agar plate culture medium. Then the membrane (5 cm²) was placed on the agar plate. After 12 h of cultivation, the size of the inhibition zone around the membranes was observed.

3. Results and discussion

3.1. Surface immobilization of ammonium/amine groups

The antibacterial RC membrane was synthesized via a one-step covalent grafting chemistry (Scheme 1). A polysiloxane network can form on the RC membrane surface by self-condensation of the silane coupling agents containing antimicrobial groups. This chemical grafting reaction involves the following steps: at first, the silane coupling agents hydrolyzed into their corresponding silanols; then, the adsorption of the hydrolyzed species adsorbed to the RC membrane surface through hydrogen bonding between silanol and cellulosic OH; finally, siloxane bridges (Si–O–Si) grafted onto cellulose membrane surface through Si–O–C bonds. The highest grafting yields were 0.24 mg/cm²,

0.34 mg/cm² and 1.12 mg/cm² for RC-QAS_{C0}, RC-QAS_{C18} and RC-NH₂, respectively. RC-QAS membranes have much lower grafting yields than RC-NH₂ membrane; this can be due to the charged groups of the QAS structure and the resulted silanols. The initially adsorbed silanols may form a charged hydrogel layer preventing further deposition of silanols due to electrostatic repulsion, leading to low adsorption of silanols and then the low grafting yields.

FTIR was used to characterize the chemical structure of the original RC membrane and the grafted RC membranes. The typical spectra of RC, RC-QAS_{C0}, RC-QAS_{C18} and RC-NH₂ membranes are shown in Fig. 1. For the spectrum of RC membrane, a prominent and wide adsorption centered at 3348 cm⁻¹ can be attributed to the OH stretching vibration. The adsorption at 1170–1050 cm⁻¹ can be assigned to the vibrations of the C–O–C bond. Apart from the typical adsorption bands of cellulose, new adsorptions appear in the spectra of RC-QAS_{C0}, RC-QAS_{C18} and RC-NH₂. An obvious increment of the band at 2880 cm⁻¹ is associated with the CH₂ stretching of the propyl moiety in the silane coupling agents. The spectra of RC-QAS_{C0} and RC-QAS_{C18} also reveal a new band at 1550 cm⁻¹, which can be attributed to the quaternary ammonium (C–N stretching) groups. For the spectrum of RC-NH₂, the presence of the adsorption at 1568 cm⁻¹ is assigned to the primary amino groups (NH₂). The Si–O–C (around 1150 cm⁻¹) and Si–O–Si bridges (around 1135 cm⁻¹) are not easily seen by FTIR. Their adsorption should be buried in the large and intense cellulose C–O–C vibration bands.

The covalent attachment of the quaternary ammonium salt and aminoalkyl groups on RC was further ascertained using XPS measurements. Fig. 2a shows the XPS wide scans of RC, RC-QAS_{C0}, RC-QAS_{C18} and RC-NH₂. Two major peaks at 284.6 eV and 535.1 eV are detected for the pristine membrane. They correspond to C1s and O1s adsorptions.

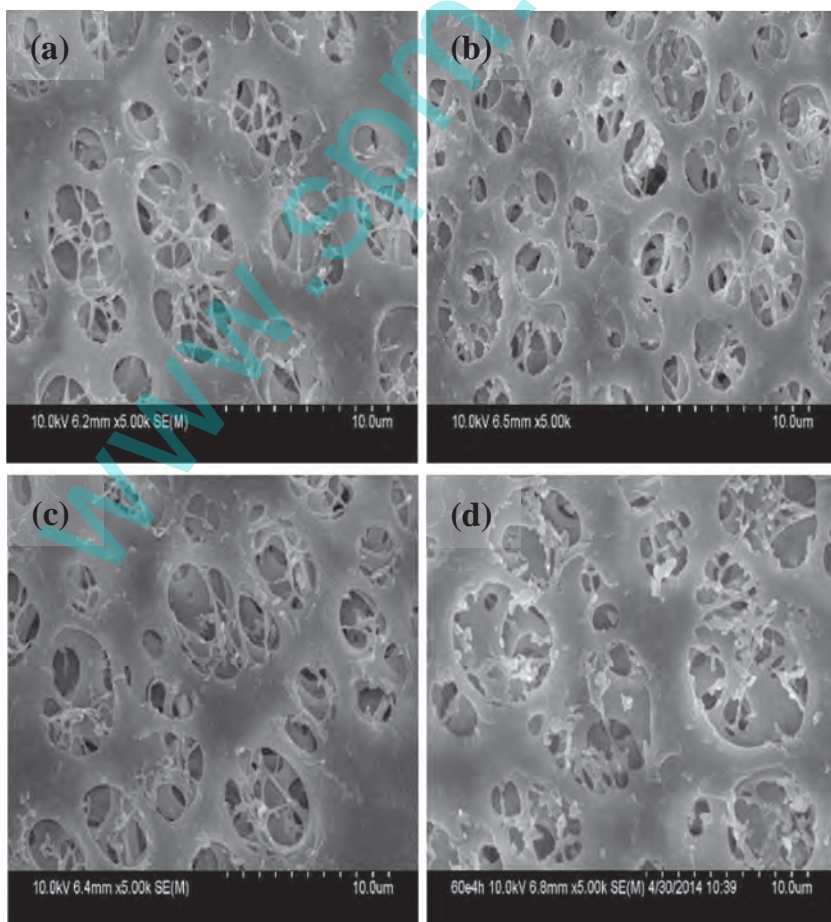


Fig. 3. SEM images of the surface morphology of the membranes RC (a), RC-QAS_{C0} (b), RC-QAS_{C18} (c) and RC-NH₂ (d) at a magnification of 5000 \times .

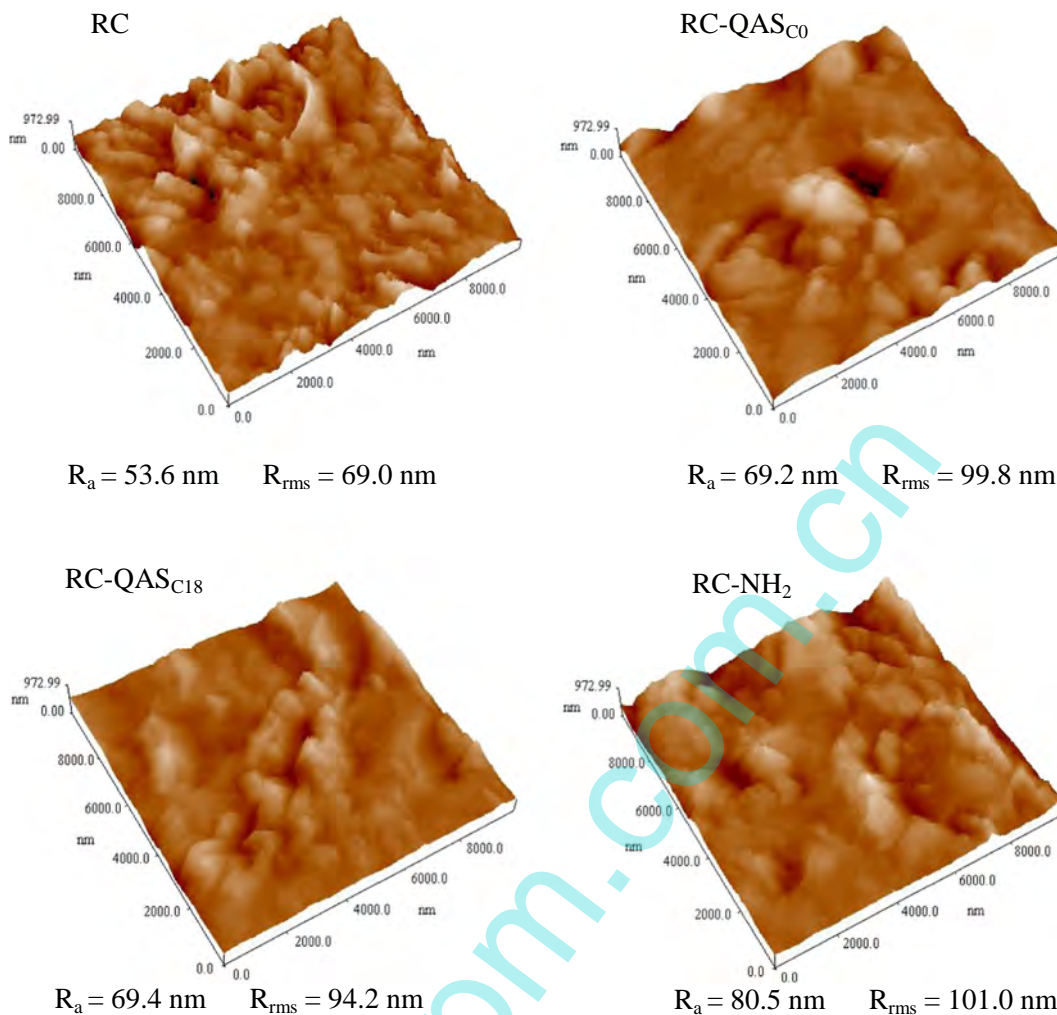


Fig. 4. AFM images of original and modified RC membranes over an area of $10 \mu\text{m} \times 10 \mu\text{m}$.

New emission peaks of N1s (402.3 eV), Si2p (100.3 eV) and Cl2p (196.9 eV) are observed for the RC-QAS_{C0} and RC-QAS_{C18} membranes. In the case of RC-NH₂ membrane, the appearance of the strong primary amine (N1s) signal at a binding energy (BE) of 400 eV and the Si2p signal at 100.3 eV is consistent with the presence of APS moieties. Fig. 2b and c shows the XPS N1s core-level spectra of the RC-QAS membranes. The N1s adsorption can be resolved into the neutral C–N peak component at 399.9 eV and the C–N⁺ peak component at 402.3 eV. The C–N⁺

peak component is the dominated specie, which suggests that the membrane surface was successfully grafted with quaternary ammonium. Fig. 2d shows the N1s core-level spectra of the RC-NH₂ surface. The NH₂ groups correspond to the peak component at 398.7 eV in the N1s spectrum. And some amino groups may also undergo H-bonding with each other or with substrate hydroxyls, as revealed by the presence of a shoulder at 400.7 eV [36]. This confirms the occurrence of RC surface NH₂-alkylation. The corresponding composition of these membrane

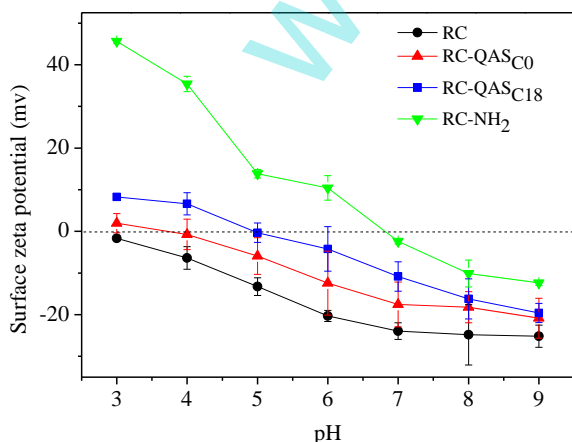


Fig. 5. The zeta potential of RC, RC-QAS_{C0}, RC-QAS_{C18} and RC-NH₂ membranes at pH of 3–9.

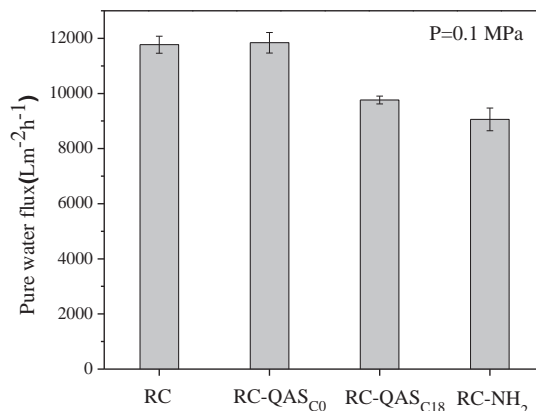


Fig. 6. The water flux of RC, RC-QAS_{C0}, RC-QAS_{C18} and RC-NH₂ membranes.

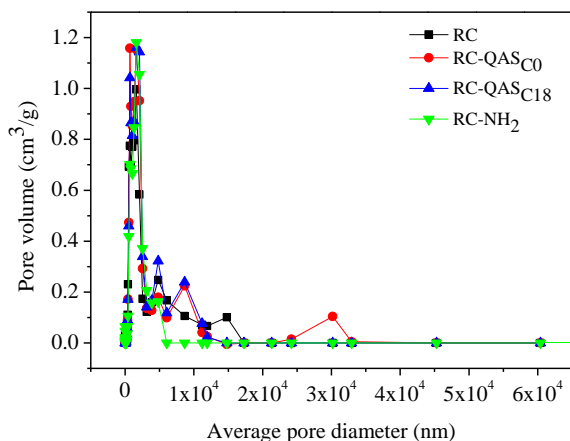


Fig. 7. The pore size distribution of RC, RC-QAS_{C0}, RC-QAS_{C18} and RC-NH₂ membranes.

surfaces is listed in Table 1. The increased carbon content is due to the silanyl group and the significant increase in the surface elemental N, Si and Cl also indicates that the RC was successfully modified with ammonium/amine groups.

The surface morphologies of the pristine and modified membrane (at magnifications of 5000 \times) are shown in Fig. 3. It can be clearly seen that the original cellulose membrane has a large average pore size which is typical for microfiltration membranes. In addition, the anchoring of antibacterial groups brings out minimal alteration on membrane surface morphology and the nascent porous structure of cellulose membrane has been preserved. The membrane surface morphology was also investigated by AFM and the results are shown in Fig. 4. The modified membranes show increased surface roughness than the pristine RC membrane. The average surface roughness (R_a) of the RC, RC-QAS_{C0}, RC-QAS_{C18} and RC-NH₂ membranes are 53.6 nm, 69.2 nm, 69.4 nm and 80.5 nm, respectively. Similar phenomenon upon surface grafting has been reported in the literature [37].

3.2. Surface wettability

The membrane surface wettability was evaluated using static water contact angle (WCA) measurements. The WCA of the RC membrane is 54.3 $^\circ$, which indicates intrinsic hydrophilicity of the cellulose membrane surface. After grafting of the different silane coupling agents, the

WCA values of the modified membranes RC-QAS_{C0}, RC-QAS_{C18} and RC-NH₂ were 48.3 $^\circ$, 91.0 $^\circ$ and 93.5 $^\circ$, respectively. Obviously, the RC and RC-QAS_{C0} membranes show much better wettability than the RC-QAS_{C18} and RC-NH₂ membranes. The WCA of RC-QAS_{C18} and RC-NH₂ membranes significantly increased due to the tethered comparatively hydrophobic alkyl and aminoalkyl groups. The surface energy of original and modified RC membranes was estimated based the WCA results using the Young–Dupré equation (Eq. (2)). The surface energies of the RC-QAS_{C18} and RC-NH₂ membranes are 71.5 mN m⁻¹ and 68.4 mN m⁻¹, respectively, which are much lower than the surface energy of RC (115.2 mN m⁻¹) and RC-QAS_{C0} (121.1 mN m⁻¹) membranes.

3.3. Surface charge properties

Surface charge properties of the original and modified RC membranes were studied by the streaming potential method over the pH range of 3.0–9.0. The results are shown in Fig. 5. It is interesting that the original RC membrane shows negative charge characteristic in the whole pH testing range. Similar results have been reported in literature [38]. This phenomenon might be caused by the adsorption of OH⁻ ions on the membrane surface via hydrogen bonding with ample hydroxyl groups in the cellulose. The modified membrane surfaces are more positively charged than the pristine RC membrane. This result can be attributed to the immobilization of the ammonium and alkylamine groups. In addition, the modified membranes show a typical amphoteric characteristic, with the positive charge at low pH contributed by the adsorption of H₃O⁺ or amine protonation and the negative charge at high pH contributed by the adsorption of OH⁻ via hydrogen bonding or ion exchange.

3.4. Permeation properties and pore size distribution

The effects of the antibacterial group immobilization on membrane permeation properties were investigated. The water flux for the pristine and modified membranes is illustrated in Fig. 6. It can be seen that the average pure water flux of the RC membrane is nearly 11,750 L m⁻² h⁻¹ at 0.1 MPa. The high flux of the RC membrane can be due to the good hydrophilicity of cellulose and the large pore size characteristic of a microfiltration membrane. The water flux of RC-QAS_{C0} slightly increased and the flux of the RC-QAS_{C18} and RC-NH₂ membranes dropped. This result can be attributed to the hydrophilicity alteration upon surface grafting and is consistent with the WCA results.

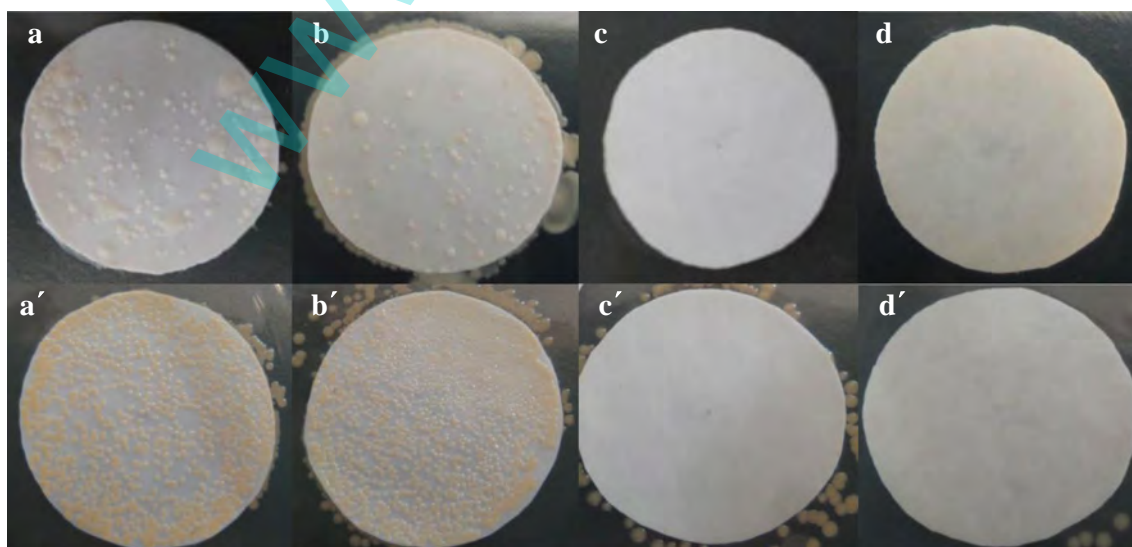


Fig. 8. Photographs showing *E. coli* (a–d) and *S. aureus* (a'–d') growth on the surfaces of RC (a, a'), RC-QAS_{C0} (b, b'), RC-QAS_{C18} (c, c') and RC-NH₂ (d, d') membranes.

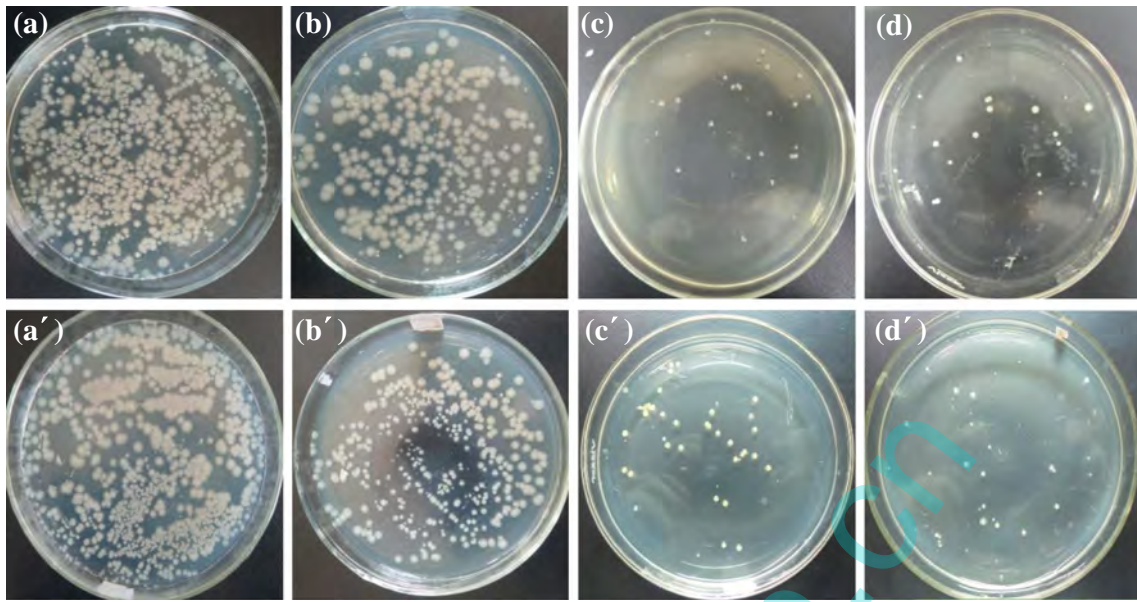


Fig. 9. Photographs of L-agar plates onto which *E. coli* (a–d) and *S. aureus* (a'–d') suspensions were treated with RC (a, a'), RC-QAS_{C0} (b, b'), RC-QAS_{C18} (c, c') and RC-NH₂ (d, d') membranes.

The mercury porosimetry was measured to investigate the effects of the surface modification on membrane pore size distribution. The results are shown in Fig. 7. It can be seen that the pore size distributions of the original and modified RC membranes range from 0.85 to 0.95 μm . Surface grafting with silane coupling agents did not cause significant alteration on the microporous structure and pore size of the RC membranes, thus bring out a minimal effect on membrane rejection properties. This result further confirmed that the membrane flux change upon grafting was primarily related to the change of surface hydrophilicity.

3.5. Antibacterial properties

E. coli and *S. aureus* were used to evaluate the bacteriostatic and bactericidal properties of the membranes. The results are presented in Fig. 8, using the pristine RC membrane as a control. It can be seen that after incubation for 12 h, the bacterial growth on RC and RC-QAS_{C0} membrane surfaces were obvious, which is especially true for the case of *S. aureus*, which almost fully cover membrane surfaces, indicating that RC and RC-QAS_{C0} had no antibacterial function. On the other hand, a significant reduction in the amount of bacterial cells was observed on RC-QAS_{C18} and RC-NH₂ surfaces. In fact, there was nearly no bacterial colony found on the membrane surfaces, which suggests the

strong antibacterial property of RC-QAS_{C18} and RC-NH₂ membranes. By comparing the results of RC-QAS_{C0} and RC-QAS_{C18} membranes, the antibacterial activity of the RC-QAS_{C18} is believed to be strongly dependent on its overall molecular structure and the length of alkyl chains. It is known that the antibacterial efficiency of ammonium groups must be assured by a long alkyl chain, which has enhanced hydrophobicity promoting penetration of ammonium groups through the hydrophobic bacterial membrane [39,40]. In the case of RC-NH₂ membrane, its strong antibacterial property compared to RC-QAS_{C18} membrane can be partially attributed to the polycationic nature of membrane surface resulted by $-\text{NH}_2$ groups [41,42]. In addition, the antimicrobial activity of RC-NH₂ can also be due to the hydrophobic propyl group which brings about lipophilic properties to the material and affect the mode of surface interaction with the cytoplasmic membrane of the bacteria [43]. By Comparing Fig. 8(a, b) with Fig. 8(a', b'), it was found that the number of *E. coli* on the membrane surface was less than the number of *S. aureus* at the same condition. This is due to the reason that *S. aureus* can form colonies more easily than *E. coli* in the same condition [44].

The effect of the introduction of quaternary ammonium salts and aminoalkyl groups onto the RC membranes on bacterial growth was also assessed by inoculating the membranes with *E. coli* and *S. aureus*. After removing the membranes from bacterial suspension, agar plates were inoculated with the bacterial suspension. The photographs of bacterial suspension after a growth for 6 h at 37 °C were shown in Fig. 9. The colony was fully developed in the case of RC and RC-QAS_{C0}, but only few colonies were observed in the case of RC-QAS_{C18} and RC-NH₂. This confirms that the RC-QAS_{C18} and RC-NH₂ membranes have an excellent antibacterial activity against both *E. coli* and *S. aureus*, while RC and RC-QAS_{C0} membranes have poor antibacterial properties. The percent viability of *E. coli* and *S. aureus* was also estimated based on the number of colonies on the agar plate. The data are presented in Fig. 10. The bacteria killing ratio of both RC-QAS_{C18} and RC-NH₂ membranes reaches more than (99.6% against *E. coli* and more than 99.5% against *S. aureus*, while RC and RC-QAS_{C0} membranes rarely have antibacterial properties, where the bacteria killing ratio is almost 0%.

3.6. Bacterial anti-adhesion properties

Bacterial anti-adhesion property of pristine RC and modified RC membranes was evaluated via a static adhesion test against *E. coli* and *S. aureus*. The membrane surfaces were observed by CLSM after

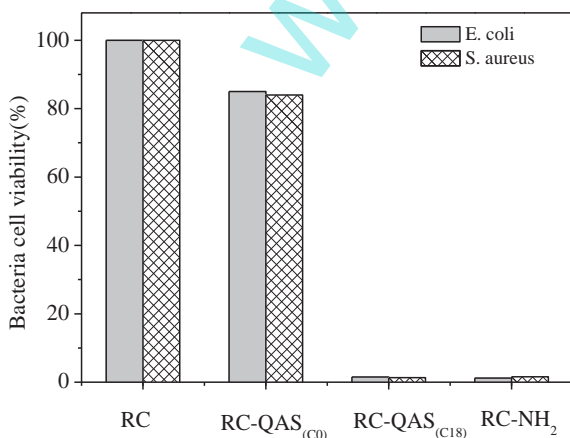


Fig. 10. Bacterial cell viability results for original and modified RC membranes.

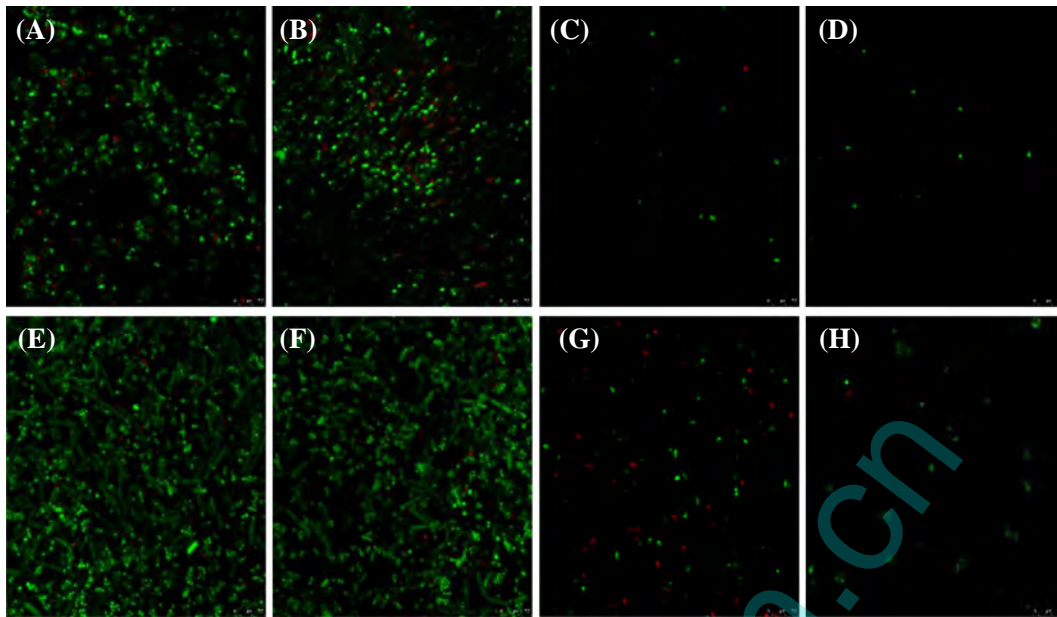


Fig. 11. Fluorescence images of live/dead stained bacteria on the membrane surface: (A–D) *E. coli* on RC, RC-QAS_{C0}, RC-QAS_{C18}, and RC-NH₂; (E–H) *S. aureus* on RC, RC-QAS_{C0}, RC-QAS_{C18}, and RC-NH₂. (For interpretation of the references to color in this figure legend, the reader is referred to the web version of this article.)

immersing in bacterial suspension for 2 days. The fluorescence images of the representative membranes after live/dead staining are shown in Fig. 11. The adhesion and growth of biofilm of both *E. coli* and *S. aureus* were much higher on RC and RC-QAS_{C0} than those on RC-QAS_{C18} and RC-NH₂ membrane surfaces, which suggest that RC-QAS_{C18} and RC-NH₂ membranes have good anti-adhesion activities. This result corresponds well with the bacterial cell viability results.

Based on the membrane surface characterization results, the strong bacterial anti-adhesion properties of RC-QAS_{C18} and RC-NH₂ membranes may be caused by the following reasons: i) the decreased surface energy upon grafting can reduce the bacteria adhesion on their surfaces; ii) both membrane surfaces can disrupt the bacterial cell membrane by a combined hydrophobic and electrostatic adsorption effect at the interface (the bacterial cell membrane is usually negatively charged). It

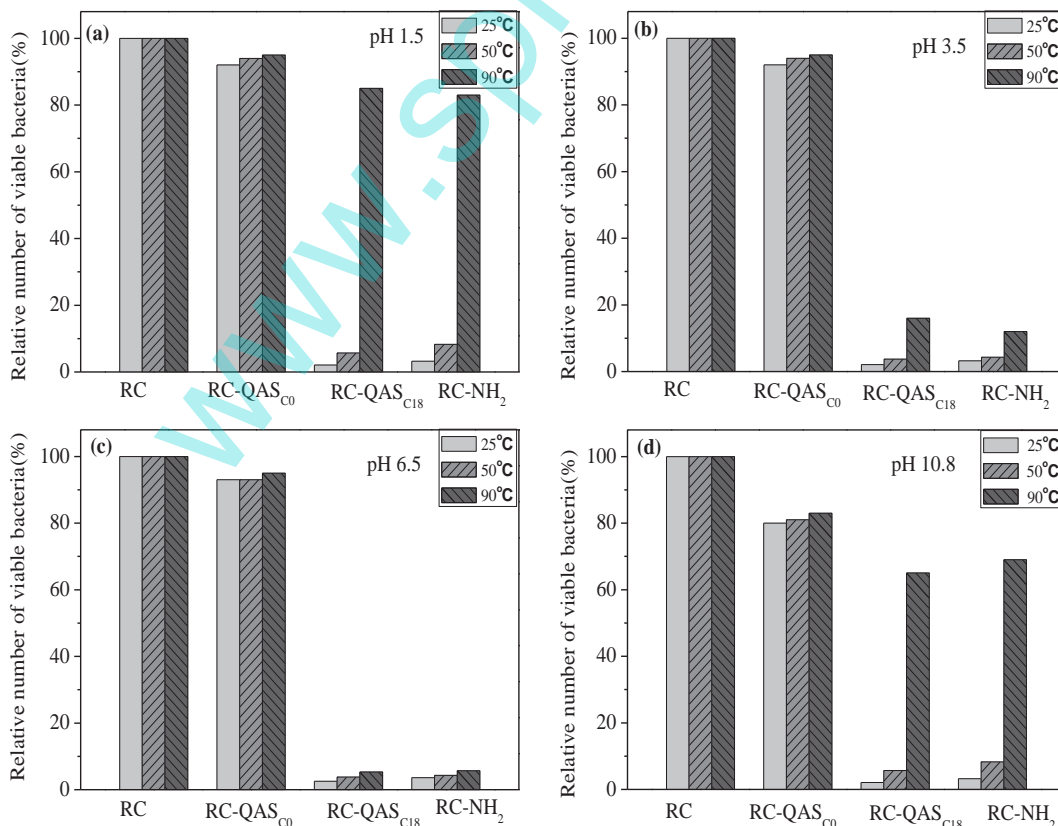


Fig. 12. Bacterial cell viability results for RC and modified RC membranes after incubation at all possible combinations of pH and temperature.

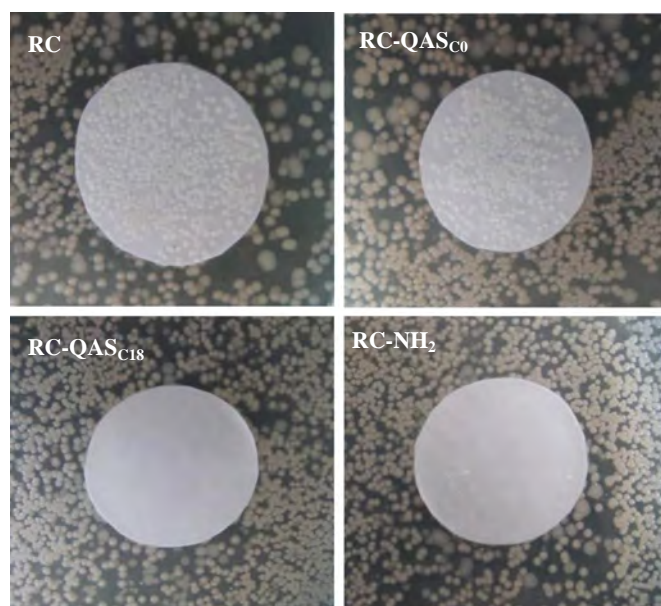


Fig. 13. Photographs of the inhibition zone test against *S. aureus*.

should be noted that the images do not allow for a quantitative measurement of the live/dead cells. However, they clearly show that the dead cells (red) on the surface of RC-QAS_{C18} and RC-NH₂ membranes.

3.7. Stability study

In order to evaluate the stability of the antimicrobial moieties, the membranes were incubated at different temperatures (25 °C, 50 °C and 90 °C) and different pHs (1.5, 3.5, 6.5 and 10.8) at all possible combinations of pH and temperature. After incubation, the CFU counting method was used to evaluate the antibacterial properties of the treated membranes. It can be found from Fig. 12 that the membranes RC-QAS_{C18} and RC-NH₂ still show a strong antibacterial activity at 25 °C and 50 °C for all pH conditions and at pH of 3.5 and 6.5 for all temperature conditions, indicating that the covalent linkage of antimicrobial agent is robust. Only at extreme conditions, such as pH of 1.5 or 10.8 at 90 °C, the bacteria viability was partially restored. Such an observation is not surprising as it is known that a combination of high temperature and highly acidic or basic conditions promotes hydrolysis of Si–O bonds [45]. However, it is difficult to envision an application in which contact active membranes need to be heated to 90 °C in a highly acidic or basic medium. Thus, the stability tests confirm the robustness of the antibacterial of modified membranes in relevant environmental pH and temperature conditions.

Fig. 13 shows the results of the diffusion inhibition zone test. The original RC and RC-QAS_{C0} membranes showed no antibacterial activity, as was evidenced by bacterial growth on the RC and RC-QAS_{C0} membrane surfaces. In contrast, nearly no bacterial cells were observed on RC-QAS_{C18} and RC-NH₂ surfaces. This result is consistent with that of Section 3.5. However, no bacteriostatic ring was observed around the membrane, thus indicating the non-leaching behavior of the antimicrobial functional groups on RC-QAS_{C18} and RC-NH₂ membrane surfaces. This result further confirmed the stable antibacterial properties of modified membranes.

4. Conclusion

In this work, an efficient and straightforward method was reported for the preparation of durable antibacterial membrane materials. Antibacterial cellulose membranes have been prepared by one-step covalent linking of quaternary ammonium salts and aminoalkyl group onto

the membrane surface via alkoxy silane polycondensation with silane coupling agents. The obtained membranes RC-QAS_{C18} and RC-NH₂ possess high bactericidal efficiency against bacteria *E. coli* and *S. aureus*. Both ammonium groups and amine groups can endow membrane robust antibacterial properties, with an adjacent hydrophobic alkyl chains as a prerequisite. The robustness of membrane resistance to bacteria has also been manifested by a stability study in a wide range of pH and temperature conditions. The evaluation of membrane antifouling performance when filtrating real fluid samples is underway in our lab and will be reported in due course.

Acknowledgments

We gratefully acknowledge the financial support by the National Natural Science Foundation of China (Grant no. 21274108), the National High Technology Research and Development Program of China (Grant no. 2012AA03A602) and Tianjin City High School Science & Technology Fund Planning Project (Grant no. 20140305) for financial support.

References

- [1] M. Ulbricht, Advanced functional polymer membranes, *Polymer* 47 (2006) 2217–2262.
- [2] P. Stroeve, N. Ileri, Biotechnical and other applications of nanoporous membranes, *Trends Biotechnol.* 29 (2011) 259–260.
- [3] A. Gugliuzza, A. Basile, Membrane Processes for Biofuel Separation: An Introduction, 3, Woodhead Publishing Limited, 2014. 65–103.
- [4] S.P. Adiga, C. Jin, L.A. Curtiss, N.A. Monteiro-Riviere, R.J. Narayan, Nanoporous membranes for medical and biological applications, *Wiley Interdiscip. Rev. Nanomed. Nanobiotechnol.* 1 (2009) 568–581.
- [5] M. Ouammou, N. Tijani, J.I. Calvo, C. Velasco, A. Martín, F. Martínez, F. Tejerina, A. Hernández, Flux decay in protein microfiltration through charged membranes as a function of pH, *Colloids Surf. A Physicochem. Eng. Asp.* 298 (2007) 267–273.
- [6] K.-J. Hwang, Y.-C. Chiang, Comparisons of membrane fouling and separation efficiency in protein/polysaccharide cross-flow microfiltration using membranes with different morphologies, *Sep. Purif. Technol.* 125 (2014) 74–82.
- [7] M. Rouabhia, J. Asselin, N. Tazi, Y. Messaddeq, D. Levinson, Z. Zhang, Production of biocompatible and antimicrobial bacterial cellulose polymers functionalized by RGDC grafting groups and gentamicin, *ACS Appl. Mater. Interfaces* 6 (2014) 1439–1446.
- [8] N. Lavoine, I. Desloges, A. Dufresne, J. Bras, Microfibrillated cellulose – its barrier properties and applications in cellulosic materials: a review, *Carbohydr. Polym.* 90 (2012) 735–764.
- [9] I. Rosas, S. Collado, A. Gutiérrez, M. Díaz, Fouling mechanisms of *Pseudomonas putida* on PES microfiltration membranes, *J. Membr. Sci.* 465 (2014) 27–33.
- [10] P. Le-Clech, V. Chen, T.A.G. Fane, Fouling in membrane bioreactors used in wastewater treatment, *J. Membr. Sci.* 284 (2006) 17–53.
- [11] A.L. Lim, R. Bai, Membrane fouling and cleaning in microfiltration of activated sludge wastewater, *J. Membr. Sci.* 216 (2003) 279–290.
- [12] A. Drews, C.H. Lee, M. Kraume, Membrane fouling – a review on the role of EPS, *Desalination* 200 (2006) 186–188.
- [13] L. Vansacker, P. Declerck, M.R. Bilad, I.F.J. Vankelecom, Biofouling on microfiltration membranes in MBRs: role of membrane type and microbial community, *J. Membr. Sci.* 453 (2014) 394–401.
- [14] B.D. Cho, A.G. Fane, Fouling transients in nominally sub-critical flux operation of a membrane bioreactor, *J. Membr. Sci.* 209 (2002) 391–403.
- [15] M. Herzberg, S. Kang, M. Elimelech, Role of extracellular polymeric substances (EPS) in biofouling of reverse osmosis membranes, *Environ. Sci. Technol.* 43 (2009) 4393–4398.
- [16] H. Nagaoka, S. Ueda, A. Miya, Influence of bacterial extracellular polymers on the membrane separation activated sludge process, *Water Sci. Technol.* 34 (1996) 165–172.
- [17] J. Huang, H. Wang, K. Zhang, Modification of PES membrane with Ag–SiO₂: reduction of biofouling and improvement of filtration performance, *Desalination* 336 (2014) 8–17.
- [18] J.A. Lichter, K.J.V. Vliet, M.F. Rubner, Design of antibacterial surfaces and interfaces: polyelectrolyte multilayers as a multifunctional platform, *Macromolecules* 42 (2009) 8573–8586.
- [19] J.A. Lichter, Assembly and Post-assembly Manipulation of Polyelectrolyte Multilayers for Control of Bacterial Attachment and Viability, 30Massachusetts Institute of Technology, Cambridge, 2009. 1–154.
- [20] S. Adibzadeh, S. Bazgir, A.A. Katbab, Fabrication and characterization of chitosan/poly(vinyl alcohol) electrospun nanofibrous membranes containing silver nanoparticles for antibacterial water filtration, *Iran. Polym. J.* 23 (2014) 645–654.
- [21] B. Jia, Y. Mei, L. Cheng, J. Zhou, L. Zhang, Preparation of copper nanoparticles coated cellulose films with antibacterial properties through one-step reduction, *ACS Appl. Mater. Interfaces* 4 (2012) 2897–2902.
- [22] K. Lewis, A.M. Klibanov, Surpassing nature: rational design of sterile-surface materials, *Trends Biotechnol.* 23 (2005) 343–348.

- [23] L. Bromberg, T.A. Hatton, Poly(N-vinylguanidine): characterization, and catalytic and bactericidal properties, *Polymer* 48 (2007) 7490–7498.
- [24] E.-R. Kenawy, S.D. Worley, R. Broughton, The chemistry and applications of antimicrobial polymers: a state-of-the-art review, *Biomacromolecules* 8 (2007) 1359–1384.
- [25] T. Thorsteinsson, M. Masson, K.G. Kristinsson, M.A. Hjalmarsdottir, H. Hilmarsson, T. Loftsson, Soft antimicrobial agents: synthesis and activity of labile environmentally friendly long chain quaternary ammonium compounds, *J. Med. Chem.* 46 (2003) 4173–4181.
- [26] J. Lin, S.K. Murthy, B.D. Olsen, K.K. Gleason, A.M. Klibanov, Making thin polymeric materials, including fabrics, microbicidal and also water-repellent, *Biotechnol. Lett.* 25 (2003) 1661–1665.
- [27] B. Dizman, M.O. Elasmri, L.J. Mathias, Synthesis and antibacterial activities of water-soluble methacrylate polymers containing quaternary ammonium compounds, *J. Polym. Sci. A Polym. Chem.* 44 (2006) 5965–5973.
- [28] S.B. Lee, R.R. Koepsel, S.W. Morley, K. Matyjaszewski, Y. Sun, A.J. Russell, Permanent, nonleaching antibacterial surfaces. 1. Synthesis by atom transfer radical polymerization, *Biomacromolecules* 5 (2004) 877–882.
- [29] S. Lenoir, C. Pagnouille, M. Galleni, P. Compere, R. Jerome, C. Detrembleur, Polyolefin matrixes with permanent antibacterial activity: preparation, antibacterial activity, and action mode of the active species, *Biomacromolecules* 7 (2006) 2291–2296.
- [30] R.L. Gettings, W.C. White, Progress in the Application of a Surface-bonded Antimicrobial, *BioProd. Div.*, Dow Corning Corp., Midland, MI, 1987.
- [31] O. Wiarachai, N. Thongchul, S. Kiatkamjornwong, V.P. Hoven, Surface-quaternized chitosan particles as an alternative and effective organic antibacterial material, *Colloids Surf. B: Biointerfaces* 92 (2012) 121–129.
- [32] C. Yao, X. Li, K.G. Neoh, Z. Shi, E.T. Kang, Antibacterial poly(D,L-lactide) (PDLLA) fibrous membranes modified with quaternary ammonium moieties, *Chin. J. Polym. Sci.* 28 (2010) 581–588.
- [33] A.E. Childress, M. Elimelech, Effect of solution chemistry on the surface charge of polymeric reverse osmosis and nanofiltration membranes, *J. Membr. Sci.* 119 (1996) 253–268.
- [34] A. Hou, M. Zhou, X. Wang, Preparation and characterization of durable antibacterial cellulose biomaterials modified with triazine derivatives, *Carbohydr. Polym.* 75 (2009) 328–332.
- [35] C.X. Liu, D.R. Zhang, Y. He, X.S. Zhao, R. Bai, Modification of membrane surface for anti-biofouling performance: effect of anti-adhesion and anti-bacteria approaches, *J. Membr. Sci.* 346 (2010) 121–130.
- [36] F. Zhang, M.P. Srinivasan, Self-assembled molecular films of aminosilanes and their immobilization capacities, *Langmuir* 20 (2004) 2309–2314.
- [37] M. Wang, J. Yuan, X.B. Huang, X.M. Cai, L. Li, J. Shen, Grafting of carboxybetaine brush onto cellulose membranes via surface-initiated ARGET-ATRP for improving blood compatibility, *Colloids Surf. B: Biointerfaces* 103 (2013) 52–58.
- [38] R.Ch. Ong, T.S. Chung, J.S. de Wit, B.J. Helmer, Novel cellulose ester substrates for high performance flat-sheet thin-film composite (TFC) forward osmosis (FO) membranes, *J. Membr. Sci.* 473 (2015) 63–71.
- [39] P. Majumdar, E. Lee, N. Patel, S.J. Stafslin, J. Daniels, B.J. Chisholm, Development of environmentally friendly, antifouling coatings based on tethered quaternary ammonium salts in a crosslinked polydimethylsiloxane matrix, *J. Coat. Technol. Res.* 5 (2008) 405–417.
- [40] I. Yudovin-Farber, N. Beyth, E.I. Weiss, A.J. Domb, Antibacterial effect of composite resins containing quaternary ammonium polyethyleneimine nanoparticles, *J. Nanopart. Res.* 12 (2010) 591–603.
- [41] T. Tashiro, Antibacterial and bacterium adsorbing macromolecules, *Macromol. Mater. Eng.* 286 (2001) 63–87.
- [42] I.M. Helander, E.L. Nurmiaho-Lassila, R. Ahvenainen, J. Rhoades, S. Roller, Chitosan disrupts the barrier properties of the outer membrane of gram-negative bacteria, *Int. J. Food Microbiol.* 71 (2001) 235–244.
- [43] J.W. Rhim, S.I. Hong, H.M. Park, P.K.W. Ng, Preparation and characterization of chitosan-based nanocomposite films with antimicrobial activity, *J. Agric. Food Chem.* 54 (2006) 5814–5822.
- [44] K. Hamed, T. Ryosuke, O. Yoshikage, M. Hideto, Enhancing the antibiofouling performance of RO membranes using Cu(OH)₂ as an antibacterial agent, *Desalination* 325 (2013) 40–47.
- [45] P.H. Karkhanechi, R. Takagi, Y. Ohmukai, H. Matsuyama, Durable contact active antimicrobial materials formed by a one-step covalent modification of polyvinyl alcohol, cellulose and glass surfaces, *Colloids Surf. B: Biointerfaces* 112 (2013) 356–361.